University of Zagreb

Doctoral Thesis

Measurement of the cross section for associated production of a W boson and two b quarks with the CMS detector at the Large Hadron Collider

Author:
Jelena Luetic

Supervisor:
Dr. Vuko Brigljevic

A thesis submitted in fulfilment of the requirements for the degree of Doctor of Philosophy

in the

Research Group Name
Faculty of Science

February 2015

"Thanks to my solid academic training, today I can write hundreds of words on virtually any topic without possessing a shred of information, which is how I got a good job in journalism."

Dave Barry

UNIVERSITY OF ZAGREB

Abstract

Faculty Name
Faculty of Science

Doctor of Philosophy

Measurement of the cross section for associated production of a W boson and two b quarks with the CMS detector at the Large Hadron Collider

by Jelena Luetic

The Thesis Abstract is written here (and usually kept to just this page). The page is kept centered vertically so can expand into the blank space above the title too...

Acknowledgements

The acknowledgements and the people to thank go here, don't forget to include your project advisor...

Contents

List of Figures

List of Tables

For my Gogi.

Chapter 1

Introduction

Chapter 2

Theoretical overview

Standard model of elementary particles is a theory emerged in 1960s and 1970s describing all of the known elementary particles and interactions except gravity. The final formulation of Standard model incorporates several theories: quantum electrodynamics, Glashow-Weinberg-Salam theory of electroweak processes and quantum chromodynamics, all of them describing the relations between quarks and fermions. First steps towards formulation of Standard model occurred in 1960. when Sheldon Glashow unified electromagnetic and weak interactions. In 1967. Steven Weinberg and Abdul Salam are using Higgs mechanism in the electroweak theory explaining the origin of mass for elementary particles. After discovery of neutral currents which arise from the exchange of the neutal Z boson, electroweak theory becomes generally accepted. W and Z bosons were discovered in 1981 at CERN, and their masses were in agreement with the Standard model prediction. Theory describing strong interactions got itćs final form in 1974. when it was shown that hadrons are consisting of quarks. There are evidences which show the Standard model is not a final theory of elementary particles, but so far it's predictions were confirmed every time through numerous experimental tests. Standard model has one additional nice property, all fundamental interactions arise from one general principle, the requirement of local gauge invariance.

In this chapter a brief overview of the standard model particles and interactions will be

shown with the emphasis on the W boson and b quarks which are the most relevant for this thesis. Cross section determination at hadron colliders will be shown. In the last part of the chapter historical account of the development of W+b-jets theoretical calculations is described together with the existing experimental results.

2.1 Standard model overview

Elementary particle physics is described within a framework of Standard Model. We usually imagine particles as point like objects and some forces between them. Particles, or matter, are fermions, leptons of quarks of spin $s = 1/2$. There are three charged leptons, electron, muon and tau which properties are the same except for their mass. Each of the leptons has a corresponding neutrally charged neutrino which has a very small mass. There are six different types of quarks with charge either $Q = 2/3$ of $Q = -1/3$. They also carry one additional quantum number which is color charge. All objects observed in nature are colorless giving raise to the concept of quark confinement. Colorless composite objects are classifies into two categories. Bayons are fermions which are made out of three quarks, for example proton or neutron. The other category are mesons which are made of two quarks like pions. Matter is divided into three categories which are identical except for the masses of the particles.

From the point of view of the quantum field theory, Standard Model is based on a gauge symmetry $SU(3)_C \times SU(2)_L \times U(1)_Y$. Strong interaction is described by $SU(3)_C$, while electroweak sector is described by $SU(2)_L \times U(1)_Y$. All interactions within Standard model are mediated by an elementary particle which is a spin 1 boson. In the case of electromagnetic interaction, mediator is massless photon thus the range of electromagnetic interaction is infinite. For weak force mediators are three massive bosons $W^{\pm}$ and Z and it's range is very small (10^{-16}). These four bosons are the gauge bosons of $SU(2)_L \times U(1)_Y$ group. The interaction between electroweak bosons is allowed in the Standard Model in a way that charge conservation principle remains valid. Strong force is mediated by the

exchange of 8 massless gluons which are gauge bosons for $SU(3)_C$. Although gluons are massless, the range of the strong force is not infinite. Because of the effect of confinement, the range of the strong force is approximately the size of the lightest hadrons ($10^{-}13cm$).

Scalar sector of the Standard Model has been experimentally confirmed only recently [1, 2]. The fact that weak gauge bosons are massive indicates that $SU(2)_L \times U(1)_Y$ is not a good symmetry of the vacuum. In contrast with photon being massless, $U(1)_em$ is a good symmetry of the vacuum which means that $SU(2)_L \times U(1)_Y$ electroweak symmetry is somehow spontaneously broken to $U(1)_em$ of electromagnetism. Spontaneous symmetry breaking is implemented through Higgs mechanism which gives masses to $W\pm$ and Z boson, fermions and leaves photon massless. The details of the mechanism can be found elsewhere [3] but the main point is that the mechanism also predicts a new scalar and electrically neutral particle which is called Higgs boson. The search for Higgs boson lasted few decades before finally in 2012, a new particle was discovered with mass of 125 GeV. In subsequent years, properties of this new particle have been measured and at this point, all measurements agree with Standard Model predictions for Higgs boson.

2.1.1 Bottom quarks

Bottom quark was first predicted by Makoto Kobayashi and Toshihide Maskawa in 1974 when extending Cabbibo weak mixing angle to take into account CP violation observed in neutral K mesons. [4] The name "bottom" was introduced in 1975 by Haim Harari. The bottom quark was discovered in 1977 by the Fermilab E288 experiment team led by Leon M. Lederman through the observation of Υ resonance. [5] Kobayashi and Maskawa won the 2008 Nobel Prize in Physics for their explanation of CP-violation.

At the the LHC, the main production mechanism for b quarks is through strong interaction ($g \to bb$) and top quark decay ($t \to Wb$). Every b quark, after production, goes through the process of hadronisation, forming one of the color neutral B mesons. B meson decays electromagnetically if produced in excited state to the ground state. Lowest

state B mesons decay weakly, resulting in relatively long lifetime of 1.5 ps. According to CKM matrix, b quark can decay either to c quark ($\approx 95\%$ of the cases) or u quark ($\approx 95\%$ of the cases). Long lifetime of b quark makes it possible to traverse a substantial disntance inside the detector. This fact is used in the creation of various b-tagging algorithms which are taking into account tracks originating from displaced verices, discussed in Section 4.

2.1.2 Discovery and role of W boson

W boson is one of the massive mediators of weak interaction with a mass of $m_W = 80.1$ GeV. The theory of the weak interactions got it's final form in 1968 when Sheldon Glashow, Steven Weinberg, and Abdus Salam unified a theory of electromagnetism and weak interactions. The discovery of W and Z bosons at UA1 and UA2 experiments was one of the major successes of the CERN experimental facility. Super Proton Synchrotron was the first accelerator powerful enough to produce W and Z bosons. Both collaborations reported their findings in 1983 [6, 7]. W boson at the LHC is primarily produced through quark-antiquark annihilation. In majority of the cases, W boson decays to quark-antiquark pair (66%). Other decay channels include creation a lepton and it's corresponding neutrino($\approx 10\%$ per lepton generation). This decay channel was the most important for W boson discovery and it's still essential for W boson detection at hadron colliders despite the large hadronic backgrounds.

Study of W+jets production at hadron colliders started in 1980s motivated by the top quark searches. Additional jets either come from radiation of additional quarks or gluons. However, becuse they carry color charge, quarks and gluons undergo the process of parton shower and hadronization forming jets in the detector. Parton shower is the process in which a high energy colored particle emits a low energy colored particle while hadronization is the process in which colored particle combine to form color neutral particles. Parton shower and hadronization cannot be computed analytically, but have to be modeled using Monte Carlo simulations. As a result of these processes, in the final state there can be a number of jets that doesn't correspond to the number of incoming partons.

This becomes relevant when trying to form an inclusive W+jets sample from exclusive (W + 1 jet, W + 2 jets...) samples and some process of matching has to be performed in order to avoid double counting. Matching procedure is described in detail in [8].

Many theoretical issues arise when trying to compute cross sections for W+jets processes. Divergences while calculating amplitudes come from emission of soft particles or collinear jets. These problems are solved by introducing a cut-off called factorization scale. Other divergences come from integrating higher-order loops. Usually this type of divergence is than included into renormalized coupling constant. This procedure, however introduces a certain scale dependence into the result which will be discussed further in Section 2.2.1.

2.2 Wbb at hadron collider

2.2.1 Cross sections at hadron colliders

Determining cross sections for processes at hadron collides is not an easy task. With proton being a composite object consisting of partons, it is necessary to include it's internal structure as well as the diagrams for hard scattering of interest. This means soft and hard processes are occurring in the same event. Quarks and gluons within proton interact through strong force and are described using quantum chromodynamics. Two processes make it possible to perform calculations within the QCD, asymptotic freedom and factorization theorem. Since strong force coupling constant α_s depends on the scale, for high momentum transfers ($Q >> \Lambda_{QCD} \approx 200\text{MeV}$) it becomes sufficiently small to make perturbative expansion in α_s possible. This feature is called asymptotic freedom and it is used to determine the hard process cross section. Figure 2.1 shows the results of the α_s measurements which is in complete agreement with the QCD predictions of asymptotic freedom.

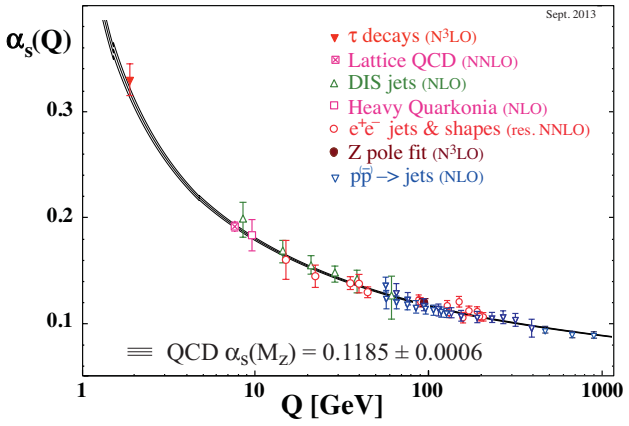

FIGURE 2.1: Summary of measurement of strong coupling constant α_s [9]

Perturbative QCD cannot be used if the momentum transfer values are small and the coupling constant becomes large. This phenomenon is called *confinement* and it requires different treatment for the quarks inside the proton. Internal structure of a proton is described using parton distribution functions which are determined through deep inelastic scattering experiments. Parton distribution functions for each of the partons inside a proton is shown in Figure 2.2 made with one specific PDF function(MSTW). Using DGLAP equations, it is possible to evolve the PDFs for any momentum transfer value which is described in detail in [10]

While performing perturbative QCD calculations, it is important to impose conditions to the final state in order to avoid soft and collinear divergences. Collinear divergences originate from configurations with a small opening angle between jets. Soft divergences appear when quark or gluon is irradiated at low momentum. Factorization scale is introduced as a cut-off for diagram calculation below which perturbative QCD calculation is not performed which means that hard scattering between partons is independent from the parton internal structure. The main point of the factorization theorem is that because of energy dependence of strong coupling constant, hard and soft part of the process are happening at different time scales ans soft part is factorized inside a parton distribution function. Drawing of a proton proton collision is shown in figure 2.3. If we want to calculate the cross section for some process where there are two protons in the

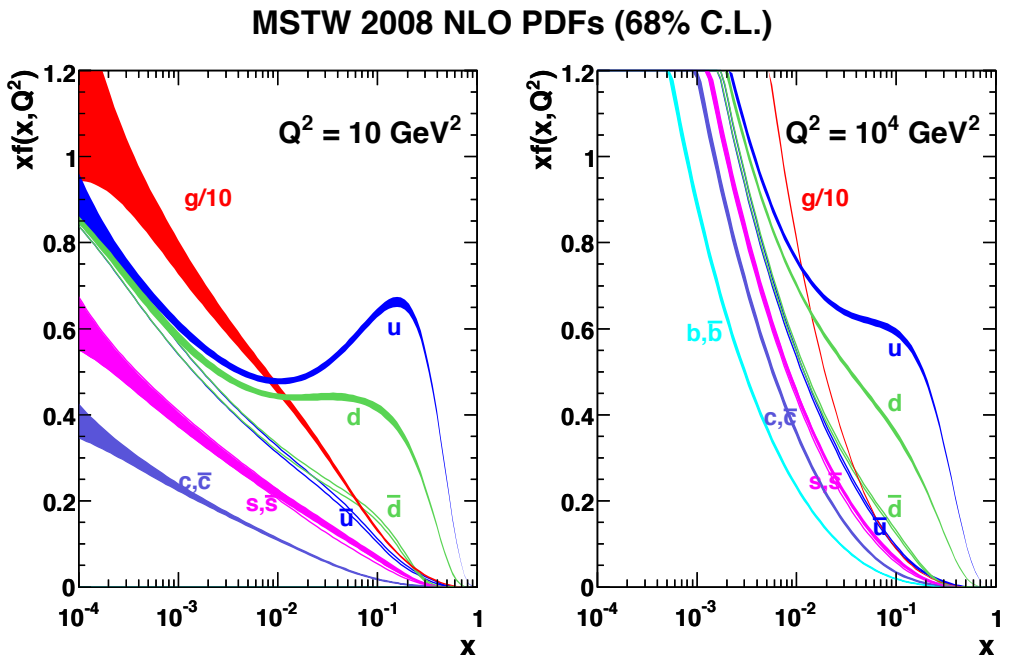

FIGURE 2.2: Parton distribution functions calculated by the MSTW group for $Q = 10\text{GeV}$ and $Q = 10^4\text{GeV}$ [11]

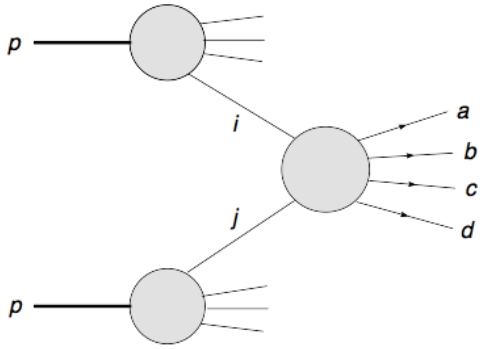

FIGURE 2.3: Drawing of a proton-proton collision.

initial state and some interesting final state which we call X, according to [10], necessary steps are:

1. Identify the leading order partonic processes that contribute to X
2. Calculate the corresponding hard scattering cross section
3. Determine the appropriate PDFs for initial state partons

4. Make a specific choices for factorization(μ_F) and renormalization(μ_R) scales

5. Perform integration over the fraction of momentum available for a given parton(x)

The cross section at hadron collides is thus a convolution of the hard scattering perturbative cross section and two incoming parton distribution functions.

$$\sigma_{AB} = \sum_{n=1}^{\infty} \alpha_s^n(\mu_R^2) \sum_{i,j} \int dx_1 dx_2 f_{i/A}(x_1, \mu_F^2) f_{j/B}(x_2, \mu_F^2) \sigma_{ij\to X}^{(n)}(x_1 x_2 s, \mu_R^2, \mu_F^2) \tag{2.1}$$

Equation 2.1 shows cross section perturbation series in α_s, n denotes the order of the series where $n = 1$ is leading order, $n = 2$ is next to leading order, etc. Hard process cross section between two partons $\sigma_{ij\to X}^{(n)}$ is computed in the framework of perturbative QCD and depends on s which is squared center of mass energy. Two parton distribution functions are denoted with $f_{i/A}$ and $f_{j/B}$ and correspond to the probability density that parton $i(j)$ with proton momentum fraction $x_1(x_2)$ will be found inside a proton. Sum over all combinations of partons has to be computed. Integral over available phase space for proton fraction momentum dx is usually carried out by simulations.
Here μ_F represents *factorization scale* and μ_R is *renormalization scale* for running coupling constant. They are arbitrary cut-offs used to remove nonperturbative effects and be able to make perturbative calculations. If cross section is computed in full series, μ_F and μ_R should cancel out, and scale dependence should disappear. However, since fewer orders are used and some residual scale dependence is still present. This dependency can be used to estimate the contribution of the missing orders in the series.

Usually factorization and renormalization scales are chosen to be identical and close to the scale of the process in question.

Figure 2.4 shows some interesting Standard model cross sections in proton-proton and proton-antiproton collisions as a function of a center of mass energy. All cross sections have been computed to the NLO order using the above described procedure.

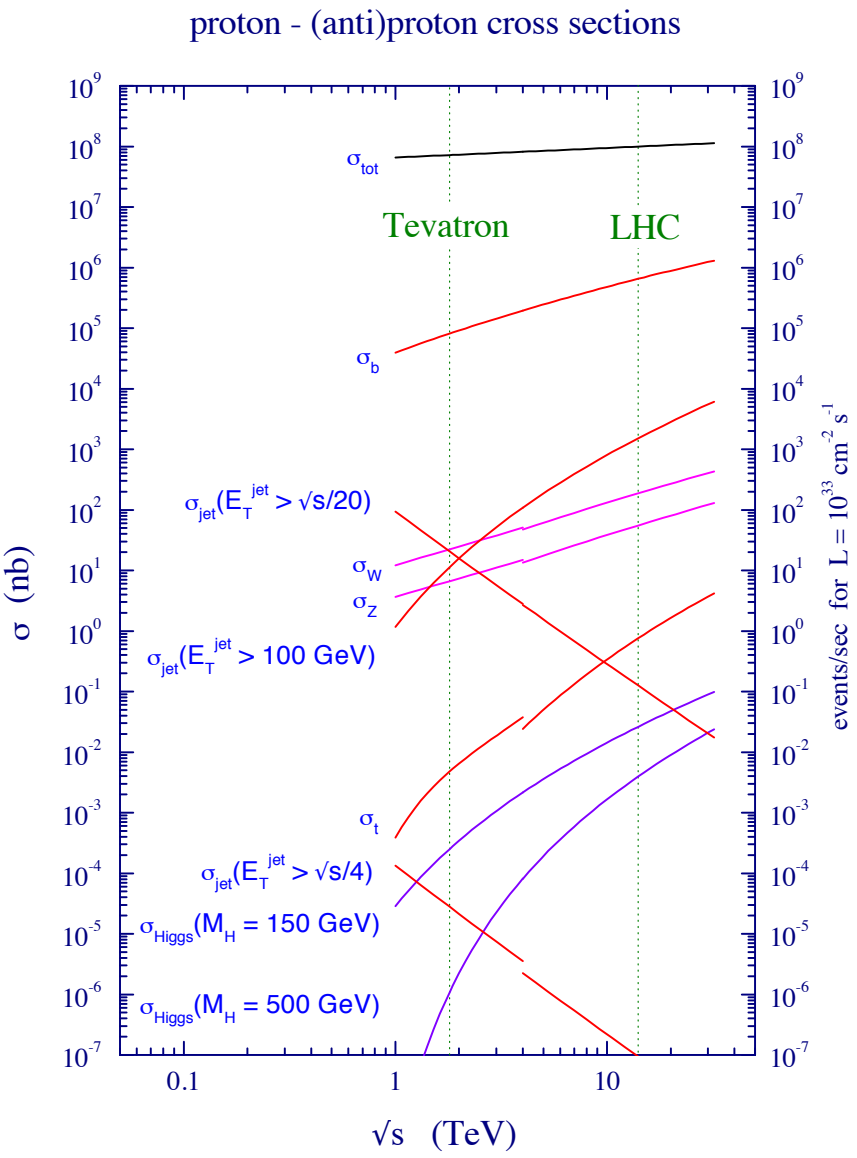

FIGURE 2.4: Standard model cross sections as a function of center of mass energy.[10]

2.2.2 Contributions to Wbb cross section

Soft and collinear divergences are naturally avoided in processes with b jets because of relatively high mass of b quark which means that the scale of the process doesn't go below $2m_b$.

2.3 Previous measurements

Previous measurements of a W boson produced in association with b quarks have been performed on different experiments. However, the final states and phase space used in these measurements were different, which means that the results cannot be directly compared, but they can be compared with theoretical predictions. This process was measured for the first time at Tevatron with D0 and CDF experiments at $\sqrt{s} = 1.96$ TeV. The CDF collaboration published its result in 2009 and the cross-section measured is that of "jets from b-quarks produced with a W boson"[12]. The event selection is based on reconstructing a leptonically decaying W boson, and one or two jets where at least one has to be b-tagged. Events with jets from light quarks are vetoed with a cut on the secondary vertex mass. Contribution of other background events containing a b quark in final state (e.g. events with top quark) is estimated using Monte Carlo simulations. The measured cross section is 2.8 standard deviations higher than corresponding theoretical prediction. D0 collaboration published their result in 2012. with somewhat different phase space definition[13]. The difference with respect to the CDF measurement consists in the inclusion of the events with 3 jets and reduced pseudorapidity range in which the measurement was performed. The measurement technique is similar to that of CDF, although b-tagging algorithms were slightly different. The measured cross section was in good agreement with the Standard model prediction.

First measurements at the LHC were published by the ATLAS collaboration based on 36/pb of integrated luminosity at $\sqrt{s} = 7$ TeV. One year later they improved their measurement using 4.6/fb [14]. Selected events contain one reconstructed electron or muon, significant amount of missing transverse energy and one or two jets where exactly one is b-tagged. The phase space is divided in two regions, depending on the number of jets. Events with exactly 2 b jets and events with more than 2 jets are vetoed in order to suppress background events from top quark decay. The results are shown in Figure 2.5. The cross section measurement in the one jet region shows an excess corresponding to 1.5 standard deviations. In the two jet region, the measured cross section is in good agreement with theoretical predictions. A differential cross section measurement as a function

of leading b jet transverse momentum has been performed for the first time and shown in figure 2.6. The cross section measurement in the one jet region is again higher that NLO predictions but within theoretical and experimental uncertainties. The cross section measured for the events with two jets is in good agreement with the theoretical prediction.

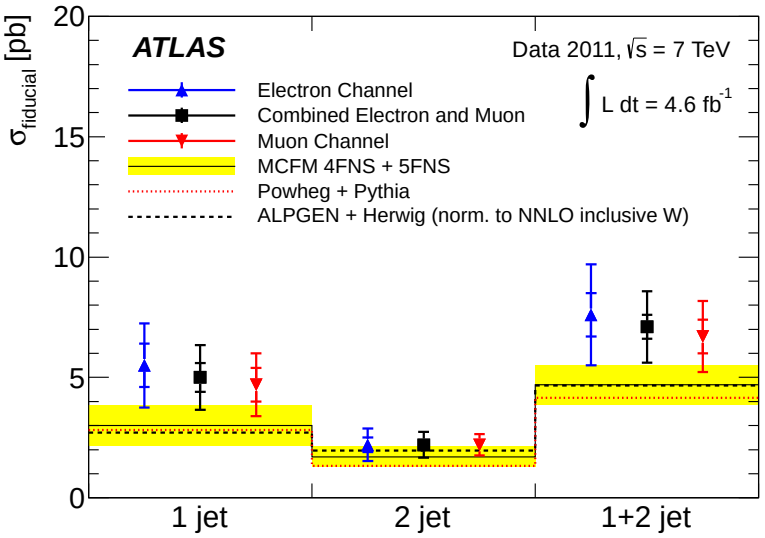

FIGURE 2.5: Measured fiducial cross-sections in the electron, muon, and combined electron and muon channels. The cross-sections are given in the 1-jet, 2-jet, and 1+2-jet fiducial regions.[14]

The CMS collaboration published its results corresponding to data collected during 2011. The measured events contained a muon and missing transverse energy in the final state, together with two b-tagged jets. The measured cross section is in excellent agreement with the Standard model prediction.[15]

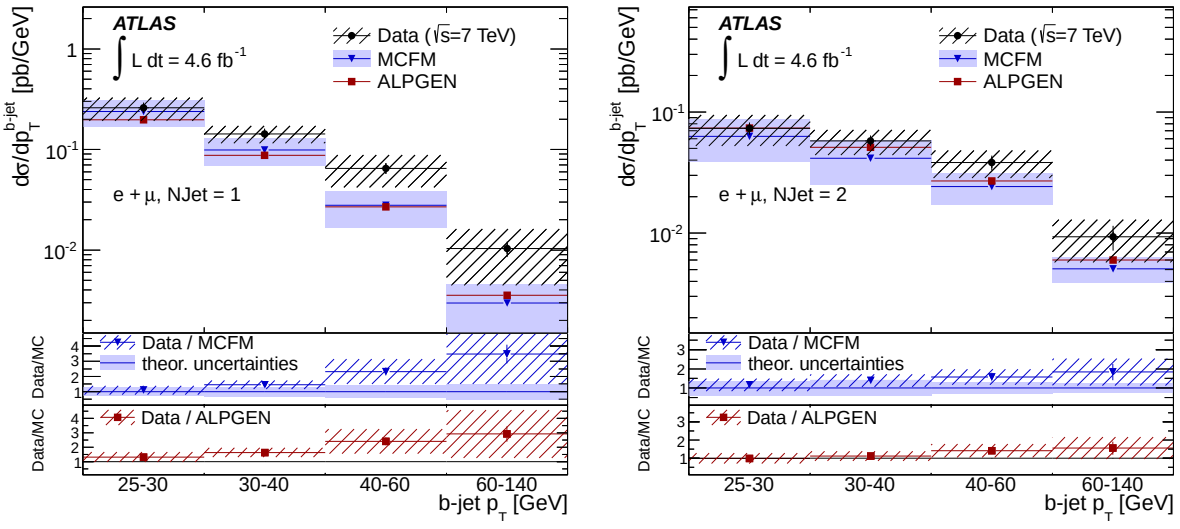

(A) (B)

FIGURE 2.6: Measured differential W+b-jets cross-sections as a function of leading b-jet p_T in the 1-jet (2.6a) and 2-jet (2.6b) fiducial regions, obtained by combining the muon and electron channel results. [14]

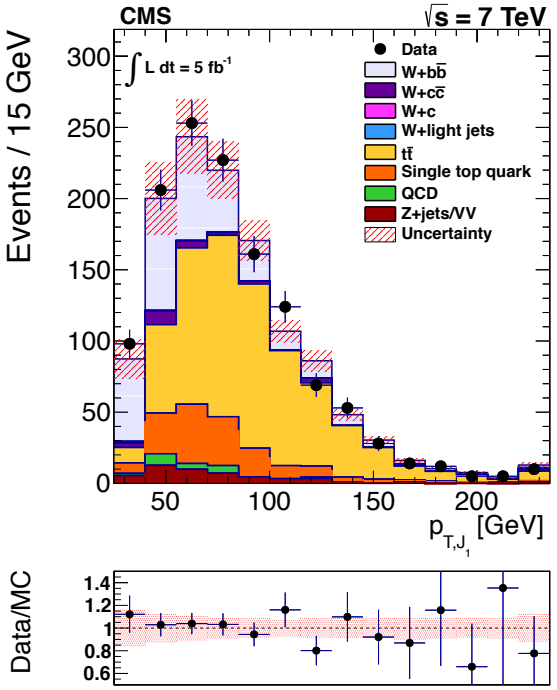

FIGURE 2.7: [15]

Chapter 3

Large Hadron Collider

3.1 Physics goals for the LHC

Lorem ipsum dolor sit amet, consectetur adipiscing elit. Aliquam ultricies lacinia euismod. Nam tempus risus in dolor rhoncus in interdum enim tincidunt. Donec vel nunc neque. In condimentum ullamcorper quam non consequat. Fusce sagittis tempor feugiat. Fusce magna erat, molestie eu convallis ut, tempus sed arcu. Quisque molestie, ante a tincidunt ullamcorper, sapien enim dignissim lacus, in semper nibh erat lobortis purus. Integer dapibus ligula ac risus convallis pellentesque.

3.1.1 Features

Nunc posuere quam at lectus tristique eu ultrices augue venenatis. Vestibulum ante ipsum primis in faucibus orci luctus et ultrices posuere cubilia Curae; Aliquam erat volutpat. Vivamus sodales tortor eget quam adipiscing in vulputate ante ullamcorper. Sed eros ante, lacinia et sollicitudin et, aliquam sit amet augue. In hac habitasse platea dictumst.

3.1.2 Collisions

Morbi rutrum odio eget arcu adipiscing sodales. Aenean et purus a est pulvinar pellentesque. Cras in elit neque, quis varius elit. Phasellus fringilla, nibh eu tempus venenatis, dolor elit posuere quam, quis adipiscing urna leo nec orci. Sed nec nulla auctor odio aliquet consequat. Ut nec nulla in ante ullamcorper aliquam at sed dolor. Phasellus fermentum magna in augue gravida cursus. Cras sed pretium lorem. Pellentesque eget ornare odio. Proin accumsan, massa viverra cursus pharetra, ipsum nisi lobortis velit, a malesuada dolor lorem eu neque.

3.2 Main Section 2

Sed ullamcorper quam eu nisl interdum at interdum enim egestas. Aliquam placerat justo sed lectus lobortis ut porta nisl porttitor. Vestibulum mi dolor, lacinia molestie gravida at, tempus vitae ligula. Donec eget quam sapien, in viverra eros. Donec pellentesque justo a massa fringilla non vestibulum metus vestibulum. Vestibulum in orci quis felis tempor lacinia. Vivamus ornare ultrices facilisis. Ut hendrerit volutpat vulputate. Morbi condimentum venenatis augue, id porta ipsum vulputate in. Curabitur luctus tempus justo. Vestibulum risus lectus, adipiscing nec condimentum quis, condimentum nec nisl. Aliquam dictum sagittis velit sed iaculis. Morbi tristique augue sit amet nulla pulvinar id facilisis ligula mollis. Nam elit libero, tincidunt ut aliquam at, molestie in quam. Aenean rhoncus vehicula hendrerit.

Chapter 4

Compact Muon Solenoid

4.1 Inner tracker system

Lorem ipsum dolor sit amet, consectetur adipiscing elit. Aliquam ultricies lacinia euismod. Nam tempus risus in dolor rhoncus in interdum enim tincidunt. Donec vel nunc neque. In condimentum ullamcorper quam non consequat. Fusce sagittis tempor feugiat. Fusce magna erat, molestie eu convallis ut, tempus sed arcu. Quisque molestie, ante a tincidunt ullamcorper, sapien enim dignissim lacus, in semper nibh erat lobortis purus. Integer dapibus ligula ac risus convallis pellentesque.

4.1.1 Pixel Detector

Nunc posuere quam at lectus tristique eu ultrices augue venenatis. Vestibulum ante ipsum primis in faucibus orci luctus et ultrices posuere cubilia Curae; Aliquam erat volutpat. Vivamus sodales tortor eget quam adipiscing in vulputate ante ullamcorper. Sed eros ante, lacinia et sollicitudin et, aliquam sit amet augue. In hac habitasse platea dictumst.

4.1.1.1 Lorentz angle measurement

4.1.2 Strip detector

Morbi rutrum odio eget arcu adipiscing sodales. Aenean et purus a est pulvinar pellentesque. Cras in elit neque, quis varius elit. Phasellus fringilla, nibh eu tempus venenatis, dolor elit posuere quam, quis adipiscing urna leo nec orci. Sed nec nulla auctor odio aliquet consequat. Ut nec nulla in ante ullamcorper aliquam at sed dolor. Phasellus fermentum magna in augue gravida cursus. Cras sed pretium lorem. Pellentesque eget ornare odio. Proin accumsan, massa viverra cursus pharetra, ipsum nisi lobortis velit, a malesuada dolor lorem eu neque.

4.2 Electromagnetic calorimeter

Sed ullamcorper quam eu nisl interdum at interdum enim egestas. Aliquam placerat justo sed lectus lobortis ut porta nisl porttitor. Vestibulum mi dolor, lacinia molestie gravida at, tempus vitae ligula. Donec eget quam sapien, in viverra eros. Donec pellentesque justo a massa fringilla non vestibulum metus vestibulum. Vestibulum in orci quis felis tempor lacinia. Vivamus ornare ultrices facilisis. Ut hendrerit volutpat vulputate. Morbi condimentum venenatis augue, id porta ipsum vulputate in. Curabitur luctus tempus justo. Vestibulum risus lectus, adipiscing nec condimentum quis, condimentum nec nisl. Aliquam dictum sagittis velit sed iaculis. Morbi tristique augue sit amet nulla pulvinar id facilisis ligula mollis. Nam elit libero, tincidunt ut aliquam at, molestie in quam. Aenean rhoncus vehicula hendrerit.

4.3 Hadronic calorimeter

4.4 Solenoid

4.5 Muon chambers

4.6 Trigger

4.7 Data acquisition system

Chapter 5

Physics objects definitions

5.1 Electrons

Lorem ipsum dolor sit amet, consectetur adipiscing elit. Aliquam ultricies lacinia euismod. Nam tempus risus in dolor rhoncus in interdum enim tincidunt. Donec vel nunc neque. In condimentum ullamcorper quam non consequat. Fusce sagittis tempor feugiat. Fusce magna erat, molestie eu convallis ut, tempus sed arcu. Quisque molestie, ante a tincidunt ullamcorper, sapien enim dignissim lacus, in semper nibh erat lobortis purus. Integer dapibus ligula ac risus convallis pellentesque.

5.1.1 Electron identification

Nunc posuere quam at lectus tristique eu ultrices augue venenatis. Vestibulum ante ipsum primis in faucibus orci luctus et ultrices posuere cubilia Curae; Aliquam erat volutpat. Vivamus sodales tortor eget quam adipiscing in vulputate ante ullamcorper. Sed eros ante, lacinia et sollicitudin et, aliquam sit amet augue. In hac habitasse platea dictumst.

5.1.2 Electron isolation

Morbi rutrum odio eget arcu adipiscing sodales. Aenean et purus a est pulvinar pellentesque. Cras in elit neque, quis varius elit. Phasellus fringilla, nibh eu tempus venenatis, dolor elit posuere quam, quis adipiscing urna leo nec orci. Sed nec nulla auctor odio aliquet consequat. Ut nec nulla in ante ullamcorper aliquam at sed dolor. Phasellus fermentum magna in augue gravida cursus. Cras sed pretium lorem. Pellentesque eget ornare odio. Proin accumsan, massa viverra cursus pharetra, ipsum nisi lobortis velit, a malesuada dolor lorem eu neque.

5.2 Muons

Sed ullamcorper quam eu nisl interdum at interdum enim egestas. Aliquam placerat justo sed lectus lobortis ut porta nisl porttitor. Vestibulum mi dolor, lacinia molestie gravida at, tempus vitae ligula. Donec eget quam sapien, in viverra eros. Donec pellentesque justo a massa fringilla non vestibulum metus vestibulum. Vestibulum in orci quis felis tempor lacinia. Vivamus ornare ultrices facilisis. Ut hendrerit volutpat vulputate. Morbi condimentum venenatis augue, id porta ipsum vulputate in. Curabitur luctus tempus justo. Vestibulum risus lectus, adipiscing nec condimentum quis, condimentum nec nisl. Aliquam dictum sagittis velit sed iaculis. Morbi tristique augue sit amet nulla pulvinar id facilisis ligula mollis. Nam elit libero, tincidunt ut aliquam at, molestie in quam. Aenean rhoncus vehicula hendrerit.

5.2.1 Muon identification

5.2.2 Muon isolation

5.3 Jets

5.3.1 Jet identification

5.3.2 Jets from b quarks

5.4 Missing transverse energy

5.5 W boson candidates

Chapter 6

Signal selection

6.1 Analysis strategy

Lorem ipsum dolor sit amet, consectetur adipiscing elit. Aliquam ultricies lacinia euismod. Nam tempus risus in dolor rhoncus in interdum enim tincidunt. Donec vel nunc neque. In condimentum ullamcorper quam non consequat. Fusce sagittis tempor feugiat. Fusce magna erat, molestie eu convallis ut, tempus sed arcu. Quisque molestie, ante a tincidunt ullamcorper, sapien enim dignissim lacus, in semper nibh erat lobortis purus. Integer dapibus ligula ac risus convallis pellentesque.

6.1.1 Subsection 1

Nunc posuere quam at lectus tristique eu ultrices augue venenatis. Vestibulum ante ipsum primis in faucibus orci luctus et ultrices posuere cubilia Curae; Aliquam erat volutpat. Vivamus sodales tortor eget quam adipiscing in vulputate ante ullamcorper. Sed eros ante, lacinia et sollicitudin et, aliquam sit amet augue. In hac habitasse platea dictumst.

6.1.2 Subsection 2

Morbi rutrum odio eget arcu adipiscing sodales. Aenean et purus a est pulvinar pellentesque. Cras in elit neque, quis varius elit. Phasellus fringilla, nibh eu tempus venenatis, dolor elit posuere quam, quis adipiscing urna leo nec orci. Sed nec nulla auctor odio aliquet consequat. Ut nec nulla in ante ullamcorper aliquam at sed dolor. Phasellus fermentum magna in augue gravida cursus. Cras sed pretium lorem. Pellentesque eget ornare odio. Proin accumsan, massa viverra cursus pharetra, ipsum nisi lobortis velit, a malesuada dolor lorem eu neque.

6.2 Background estimation

Sed ullamcorper quam eu nisl interdum at interdum enim egestas. Aliquam placerat justo sed lectus lobortis ut porta nisl porttitor. Vestibulum mi dolor, lacinia molestie gravida at, tempus vitae ligula. Donec eget quam sapien, in viverra eros. Donec pellentesque justo a massa fringilla non vestibulum metus vestibulum. Vestibulum in orci quis felis tempor lacinia. Vivamus ornare ultrices facilisis. Ut hendrerit volutpat vulputate. Morbi condimentum venenatis augue, id porta ipsum vulputate in. Curabitur luctus tempus justo. Vestibulum risus lectus, adipiscing nec condimentum quis, condimentum nec nisl. Aliquam dictum sagittis velit sed iaculis. Morbi tristique augue sit amet nulla pulvinar id facilisis ligula mollis. Nam elit libero, tincidunt ut aliquam at, molestie in quam. Aenean rhoncus vehicula hendrerit.

Chapter 7

Prosireni sazetak:

7.1 Main Section 1

Lorem ipsum dolor sit amet, consectetur adipiscing elit. Aliquam ultricies lacinia euismod. Nam tempus risus in dolor rhoncus in interdum enim tincidunt. Donec vel nunc neque. In condimentum ullamcorper quam non consequat. Fusce sagittis tempor feugiat. Fusce magna erat, molestie eu convallis ut, tempus sed arcu. Quisque molestie, ante a tincidunt ullamcorper, sapien enim dignissim lacus, in semper nibh erat lobortis purus. Integer dapibus ligula ac risus convallis pellentesque.

7.1.1 Subsection 1

Nunc posuere quam at lectus tristique eu ultrices augue venenatis. Vestibulum ante ipsum primis in faucibus orci luctus et ultrices posuere cubilia Curae; Aliquam erat volutpat. Vivamus sodales tortor eget quam adipiscing in vulputate ante ullamcorper. Sed eros ante, lacinia et sollicitudin et, aliquam sit amet augue. In hac habitasse platea dictumst.

7.1.2 Subsection 2

Morbi rutrum odio eget arcu adipiscing sodales. Aenean et purus a est pulvinar pellentesque. Cras in elit neque, quis varius elit. Phasellus fringilla, nibh eu tempus venenatis, dolor elit posuere quam, quis adipiscing urna leo nec orci. Sed nec nulla auctor odio aliquet consequat. Ut nec nulla in ante ullamcorper aliquam at sed dolor. Phasellus fermentum magna in augue gravida cursus. Cras sed pretium lorem. Pellentesque eget ornare odio. Proin accumsan, massa viverra cursus pharetra, ipsum nisi lobortis velit, a malesuada dolor lorem eu neque.

7.2 Main Section 2

Sed ullamcorper quam eu nisl interdum at interdum enim egestas. Aliquam placerat justo sed lectus lobortis ut porta nisl porttitor. Vestibulum mi dolor, lacinia molestie gravida at, tempus vitae ligula. Donec eget quam sapien, in viverra eros. Donec pellentesque justo a massa fringilla non vestibulum metus vestibulum. Vestibulum in orci quis felis tempor lacinia. Vivamus ornare ultrices facilisis. Ut hendrerit volutpat vulputate. Morbi condimentum venenatis augue, id porta ipsum vulputate in. Curabitur luctus tempus justo. Vestibulum risus lectus, adipiscing nec condimentum quis, condimentum nec nisl. Aliquam dictum sagittis velit sed iaculis. Morbi tristique augue sit amet nulla pulvinar id facilisis ligula mollis. Nam elit libero, tincidunt ut aliquam at, molestie in quam. Aenean rhoncus vehicula hendrerit.

Appendix A

Lorentz angle calculation in Pixel detector

Lorentz angle is measured by using grazing angle method described in detail in [16]. From the individual signals in the detector, using reconstruction algorithms, tracks of muon candidates are obtained. From these reconstructed track it is possible to extract the entry point (x_{reco},y_{reco}) to each layer of the detector. Distance between reconstructed entry point and the actual hit in the detector is then defined as (Δx,Δy):

$$\Delta x = x_{center} - x_{reco} \tag{A.1}$$

$$\Delta y = y_{center} - y_{reco} \tag{A.2}$$

where (x_{center},y_{center}) is the position of each individual pixel center in the observed cluster. Drift of the electrons can be determined using three impact angles defined in the following way:

$$\tan\alpha = \frac{p_z}{p_x} \tag{A.3}$$

$$\tan\beta = \frac{p_z}{p_y} \tag{A.4}$$

$$\tan\gamma = \frac{p_x}{p_y} \tag{A.5}$$

where p_x,p_y and p_z are momentum components in local coordinate system which are calculated from reconstructed track parameters (Fig. A.1).

Drift of the electrons depends on the depth at which electrons are created. Depth of the

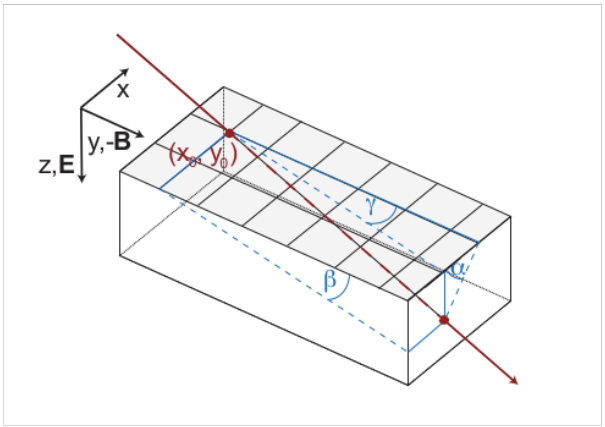

FIGURE A.1: Angle definitions for grazing angle method.

electron production z and drift due to magnetic field d are defined:

$$z = \Delta y \, \tan\beta \tag{A.6}$$

$$d = \Delta x - \Delta y \, \tan\gamma \tag{A.7}$$

This procedure is repeated for each pixel over many tracks in order to obtain charge drift distance vs depth. The Lorentz angle is the slope of this distribution. Without a magnetic field, the direction of the clusters largest extension is parallel to the track projection on the (x, y) plane. The average drift distance of an electron created at a certain depth is obtained from Fig. A.2. A linear fit is performed over the total depth of the detector excluding the first and last 50 μ where the charge drift is systematically displaced by the finite size of the pixel cell (Fig:A.3).

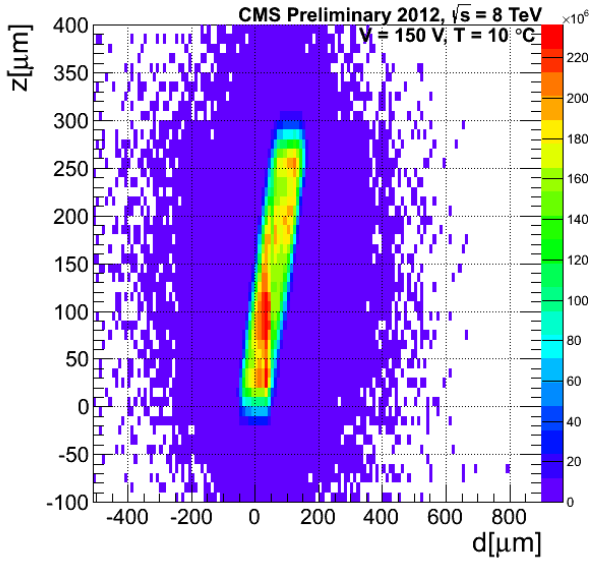

FIGURE A.2: Depth at which electrons in silicon bulk were produced as a function of Lorentz drift.

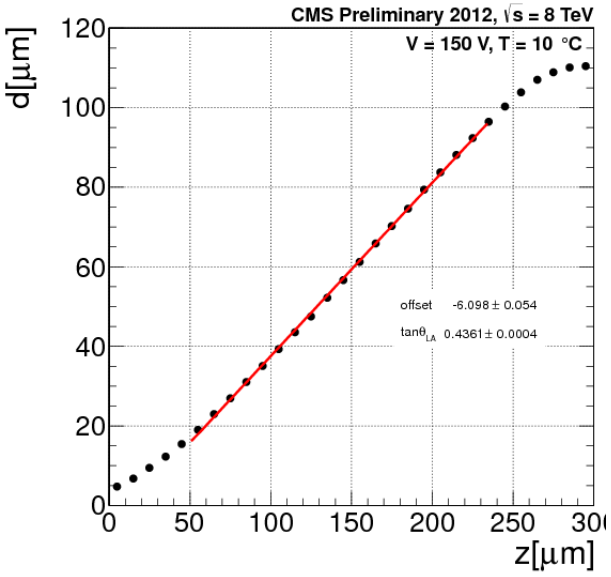

FIGURE A.3: The average drift of electrons as a function of the production depth. Slope of the linear fit result is the $tan\theta_L$.

In order to obtain a good measurement, it is important to use clean tracks. Therefore, it required to have a well reconstructed muon tracks with $p_T > 3$GeV and $\chi^2/ndof < 2$ which are required to have shallow impact angle with respect to local y direction with cluster size of at least 4 pixels in this direction. Summary of the selection criteria can be found in table A.1.

TABLE A.1: Selection criteria for Lorentz angle measurement

Cluster size in y	> 3
Track p_t	> 3GeV/c
χ^2/ndof	< 2
Hit residuals	$< 50\mu m$
Cluster charge	< 120000e

Figure A.4 shows how Lorentz angle changes with integrated luminosity. Results are shown for 23fb^{-1} of delivered luminosity in 2012. Increase in Lorentz angle measured with grazing angle method has been observed in all layers, with largest effect (6%) visible in layer 1 over this period of data taking.

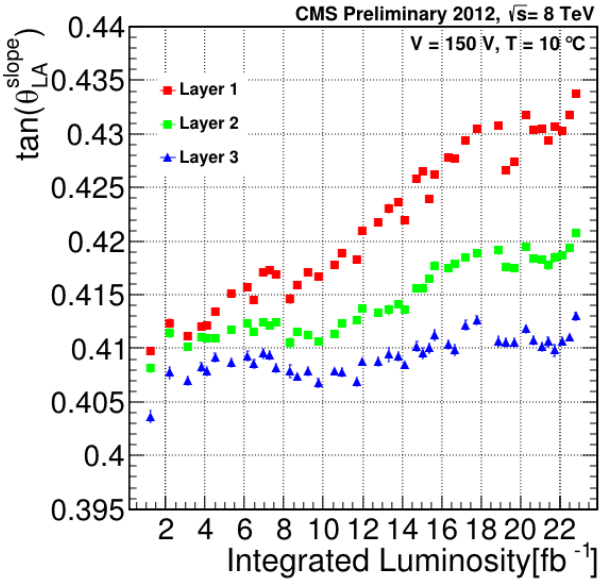

FIGURE A.4: Lorentz angle as a function of integrated luminosity for 2012.

Bibliography

[1] Georges Aad et al. Observation of a new particle in the search for the Standard Model Higgs boson with the ATLAS detector at the LHC. *Phys.Lett.*, B716:1–29, 2012.

[2] Serguei Chatrchyan et al. Observation of a new boson at a mass of 125 GeV with the CMS experiment at the LHC. *Phys.Lett.*, B716:30–61, 2012.

[3] D. Griffiths. *Introduction to Elementary Particles*. John Wiley & Sons, New York, USA, 1987.

[4] Makoto Kobayashi and Toshihide Maskawa. CP Violation in the Renormalizable Theory of Weak Interaction. *Prog.Theor.Phys.*, 49:652–657, 1973.

[5] S. W. Herb, D. C. Hom, L. M. Lederman, J. C. Sens, H. D. Snyder, J. K. Yoh, J. A. Appel, B. C. Brown, C. N. Brown, W. R. Innes, K. Ueno, T. Yamanouchi, A. S. Ito, H. Jöstlein, D. M. Kaplan, and R. D. Kephart. Observation of a dimuon resonance at 9.5 gev in 400-gev proton-nucleus collisions. *Phys. Rev. Lett.*, 39:252–255, Aug 1977.

[6] G. Arnison et al. Experimental Observation of Isolated Large Transverse Energy Electrons with Associated Missing Energy at s**(1/2) = 540-GeV. *Phys.Lett.*, B122:103–116, 1983.

[7] M. Banner et al. Observation of Single Isolated Electrons of High Transverse Momentum in Events with Missing Transverse Energy at the CERN anti-p p Collider. *Phys.Lett.*, B122:476–485, 1983.

[8] John M. Campbell. Overview of the theory of W/Z + jets and heavy flavor. 2008.

[9] K.A. Olive et al. Review of Particle Physics. *Chin.Phys.*, C38:090001, 2014.

[10] John M. Campbell, J.W. Huston, and W.J. Stirling. Hard Interactions of Quarks and Gluons: A Primer for LHC Physics. *Rept.Prog.Phys.*, 70:89, 2007.

[11] A.D. Martin, W.J. Stirling, R.S. Thorne, and G. Watt. Parton distributions for the LHC. *Eur.Phys.J.*, C63:189–285, 2009.

[12] T. Aaltonen et al. First Measurement of the b-jet Cross Section in Events with a W Boson in p anti-p Collisions at s**(1/2) = 1.96-TeV. *Phys.Rev.Lett.*, 104:131801, 2010.

[13] V.M. Abazov et al. Measurement of the $p\bar{p} \to W + b + X$ production cross section at $\sqrt{s} = 1.96$ TeV. *Phys.Lett.*, B718:1314–1320, 2013.

[14] Georges Aad et al. Measurement of the cross-section for W boson production in association with b-jets in pp collisions at $\sqrt{s} = 7$ TeV with the ATLAS detector. *JHEP*, 1306:084, 2013.

[15] Serguei Chatrchyan et al. Measurement of the production cross section for a W boson and two b jets in pp collisions at $\sqrt{s}$=7 TeV. *Phys.Lett.*, B735:204–225, 2014.

[16] B Henrich and R Kaufmann. Lorentz-angle in irradiated silicon. *Nucl. Instrum. Methods Phys. Res., A*, 477(1-3):304–307, 2002.